Article ID: 1003 - 6326(1999)04 - 0659 - 09

Solidification characteristics of near rapid and supercooling directional solidification①

Fu Hengzhi(傅恒志), Xie Faqin(谢发勤)
State Key Laboratory of Solidification Processing, Northwestern Polytechnical University, Xi'an 710072, P. R. China

Abstract: Comparing the solidification characteristics of supercooling directional solidification (SDS) with constrained directional solidification (D.S.) and considering the inheritance of supercooled melt, the supercooling directional solidification technique with the combination of melt supercooling and traditional directional solidification was proposed. An exploring study on SDS techniques was also conducted by using appropriate self-made facilities and the deep supercooling of Cu-5.0% Ni alloy and its directional solidification were implemented. The experimental results show that: 1) the solidification microstructure produced by SDS are nearly the same as that by LMC technique, its primary arm spacing is around 30 μm in average and the secondary side-branch is considerably degenerated; 2) the primary arm trunk of microstructure appears straight and fine, and the average deviation of crystal growth orientation from the axial line is about 5.8°; 3) a mathematical model describing the relationship between melt supercooling by SDS and the solidification rate, namely T-T model, was established, by which the microstructure evolution in SDS can be explained.

Key words: alloy melt; solidification characteristics; supercooling directional solidification
Document code: A

1 INTRODUCTION

Traditional D.S., such as HRS, LMC and zone melting liquid metal cooling D. S. techniques are conducted with a temperature gradient $G_L > 0$ at the head of S-L interface, and can obtain a fine or superfine dendritic microstructure. In the recent years, with the development of deep supercooling and supercooling solidification technique the solidification behavior of melt under supercooled state with $G_L > 0$ at the S-L interface, has caused great attentions. In the early 1980s, Lux[1] investigated the dynamic supercooling solidification of superalloys. In 1989, Kiminiami and others[2] predicted that after a series of study on solidification process for supercooled $Pd_{77.5}Cu_6Si_{16.5}$ there will appear a special rapid solidification technology if the traditional D.S. technique is put into combination with the melt supercooling. In 1992, Stanescu[3], based on the above consideration, proposed Autonomous Directional Solidification (ADS) technique and put it into use for the study on single crystal growth for turbine blades. Although ADS technique combined the melt supercooling with D.S., the substantial behavior of the technology is supposed to repress the nucleation of melt by changing the cooling rate, and obtain a dynamic supercooling (undercooling) (Max. of T_K near 80 K), therefore, it is still considered a mode of "dynamical solidification of supercooled melt".

In view of the above considerations, the present work is dealing with the nucleation and crystal growth mechanism during D.S. of supercooled melt at relatively lower growth rates, which is obtained by using superheat and glass purifying method to achieve a thermodynamic deep supercooling of the melt in order to reveal

① Project 59471049 supported by the National Natural Science Foundation of China and project 93G5071 supported by the Aeronautics Science Fund of China
Received Sep. 17, 1998; accepted Apr. 30, 1999

the nature of directional crystal growth of supercooled melt at $G_L<0$ in front of the S-L interface. This new technology can be called Supercooling Directional Solidification (SDS) technique[4].

2 CONSTRAINED DIRECTIONAL SOLIDIFICATION

Traditional directional solidification for making turbine blade castings is characterized by one-dimensional heat flow, positive temperature gradient at S-L interface and parallel crystal growth direction with the heat flow. For constrained D.S. growth, the well-known constitutional supercooling theory proposed by Tiller *et al*[5] is used to determine the interface stability

$$G/v = \Delta T/D \quad (1)$$

As the ratio of temperature gradient to growth rate on the left hand of Eq. (1) is less than the ratio on the right hand, there will occur constitutional suprecooling (C.S.) and interface instability, and the planar interface will transform to cellular structure. With the increase of C.S. cellular the interface becomes dendritic. Fig. 1 shows the relationship of interface morphology with respect to G_L and v.

For given alloys, the interface morphology depends on two parameters G_L/v and $G_L \cdot v$. The former mainly determines the morphology and the latter generally determines the microstructure including arm spacing. Fig. 2 gives the morphology evolution and solidification microstructure of single crystal superalloy by using conventional and high temperature gradient D.S. apparatus. It demonstrates the response of microstructure and the changes of interface morphologies to G_L/v and $G_L \cdot v$, and the appropriate rupture life at high temperature (Fig. 3). The results show that with the increase of cooling rate ($G_L \cdot v$), the changes of interface morphologies from coarse dendrites with developed sidebranches to fine dendrites and even superfine dendritic-cellular structure which leads to a corresponding increase of mechanical properties. However, the temperature gradient of the popularly used directional solidification apparatus for single crystal turbine blade is about 100 $K \cdot cm^{-1}$, so its microstructure appears coarse dendrites, as shown in Fig.2(d). Therefore, to increase the temperature gradient at the S-L interface is still considered one of the key techniques to further improve the single crystal superalloys. Practically, in the recent 30 a, continuous improvement of technology from power down, HRS and LMC could be attributed to the increase of temperature gradient, which will still be the aim of development of D.S. technique.

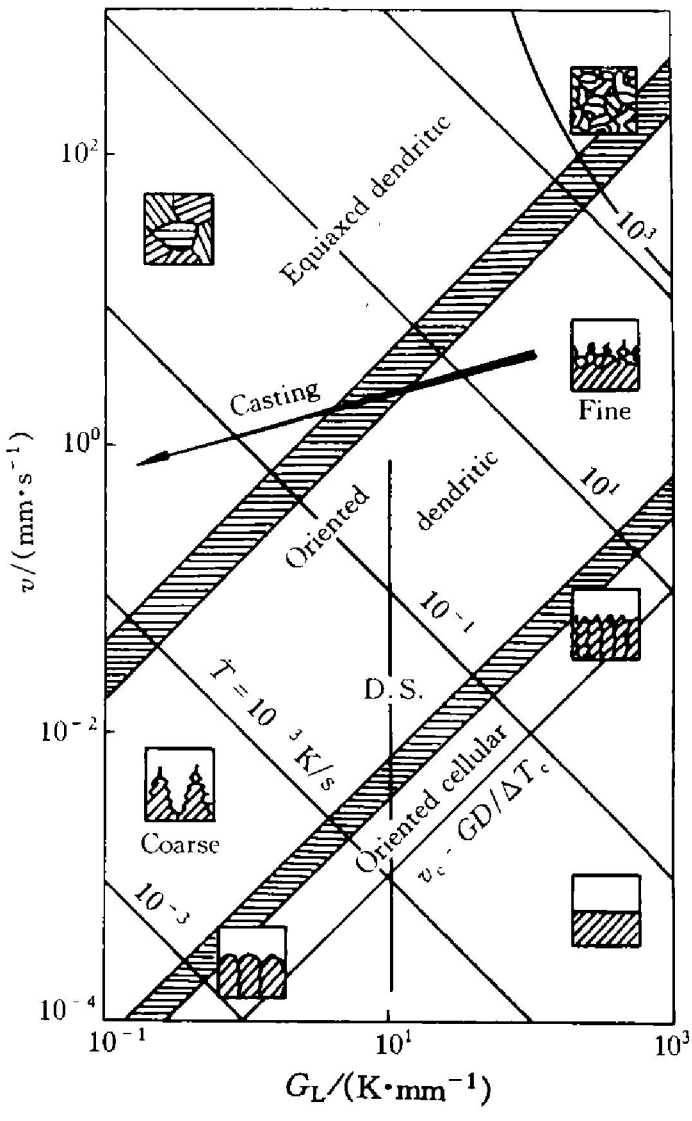

Fig.1 Relationship of interface morphology with respect to G_L and v

3 DEEP SUPERCOOLING DIRECTIONAL SOLIDIFICATION

Comparing the traditional D.S. with supercooling D.S., it can be seen that the substantial difference is that $G_L>0$ for the former, in which the heat loss depends only on the conduc-

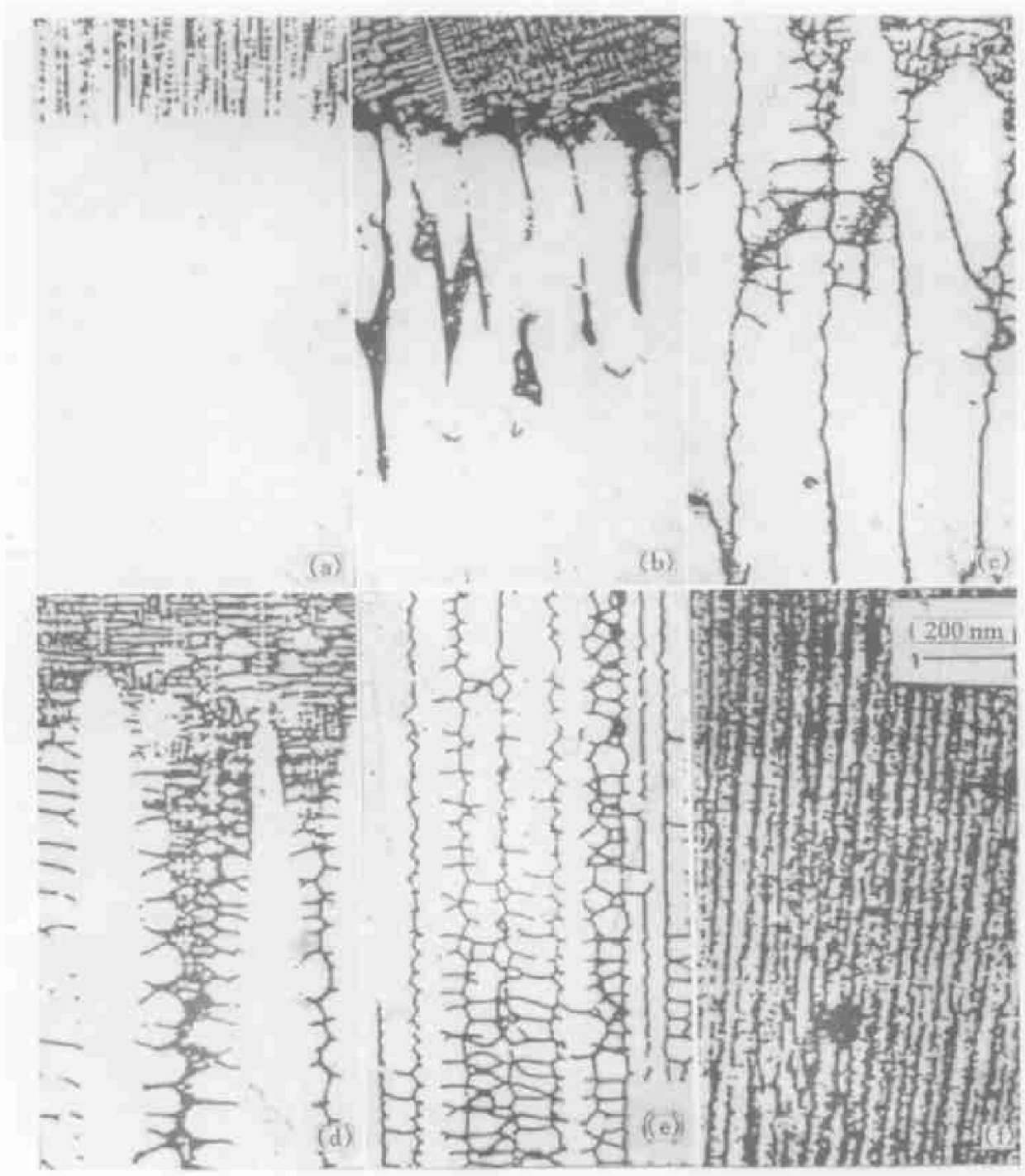

Fig.2 Morphological evolution and solidification microstructure of superalloy prepared by N1 alloy using conventional and high temperature gradient D.S. apparatus

(a)— $v=0.13\,\mu m\cdot s^{-1}$, $G_L=200K\cdot cm^{-1}$, $G_L\cdot v=2.6\times10^{-3}\,K\cdot s^{-1}$
(b)— $v=0.33\,\mu m\cdot s^{-1}$, $G_L=200K\cdot cm^{-1}$, $G_L\cdot v=6.6\times10^{-3}\,K\cdot s^{-1}$
(c)— $v=5.50\,\mu m\cdot s^{-1}$, $G_L=200\,K\cdot cm^{-1}$, $G_L\cdot v=1.1\times10^{-1}\,K\cdot s^{-1}$
(d)— $v=6.67\,\mu m\cdot s^{-1}$, $G_L=200\,K\cdot cm^{-1}$, $G_L\cdot v=2.7\times10^{-1}\,K\cdot s^{-1}$
(e)— $v=100\,\mu m\cdot s^{-1}$, $G_L=200\,K\cdot cm^{-1}$, $G_L\cdot v=2.0\times10^{0}\,K\cdot s^{-1}$
(f)— $v=100\,\mu m\cdot s^{-1}$, $G_L=1000\,K\cdot cm^{-1}$, $G_L\cdot v=10\times10^{0}\,K\cdot s^{-1}$

tion of solidified part, tip undercooling approaches to zero, but $G_L<0$, for the latter, in which the heat loss is determined both by the solidified part and the supercooled melt, and the dendritic tip undercooling can reach several to hundreds degree according to the requirement. Fig.4 shows their basic differences[1].

3.1 Methods of experiments

A quartz crucible with samples and cleaner was put into a high frequency suspension inductor and superheated circularly to eliminate the

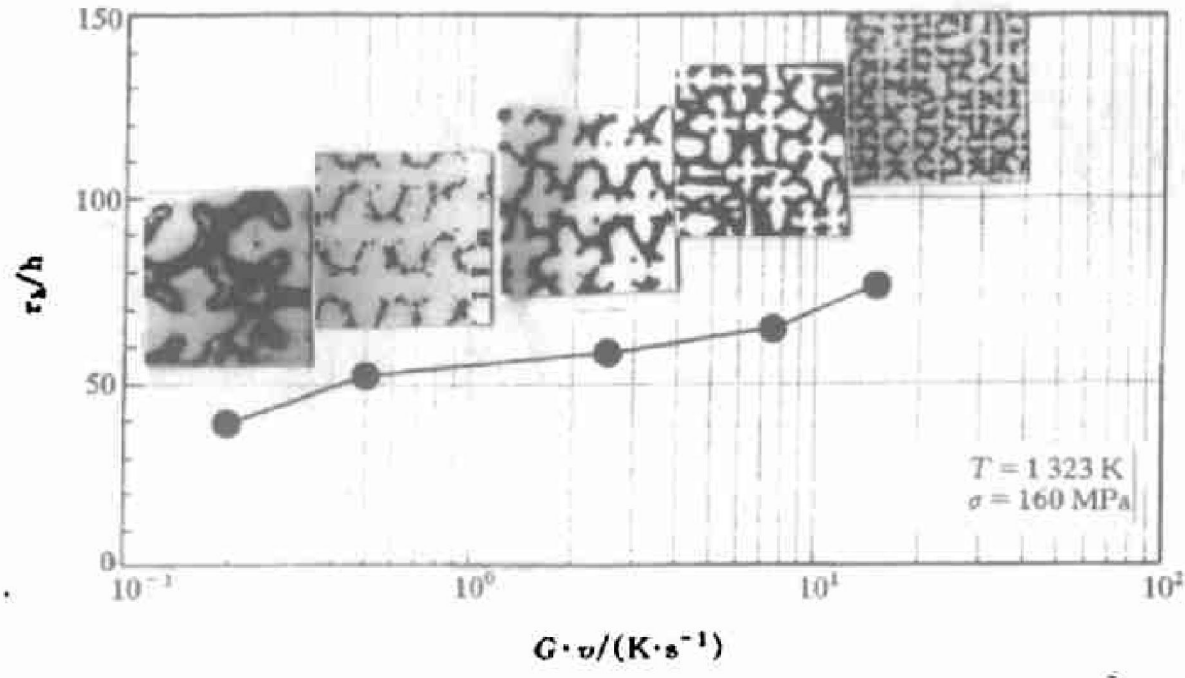

Fig. 3 Stress rupture lives of CMSX-2 at as-cast state vs cooling rate

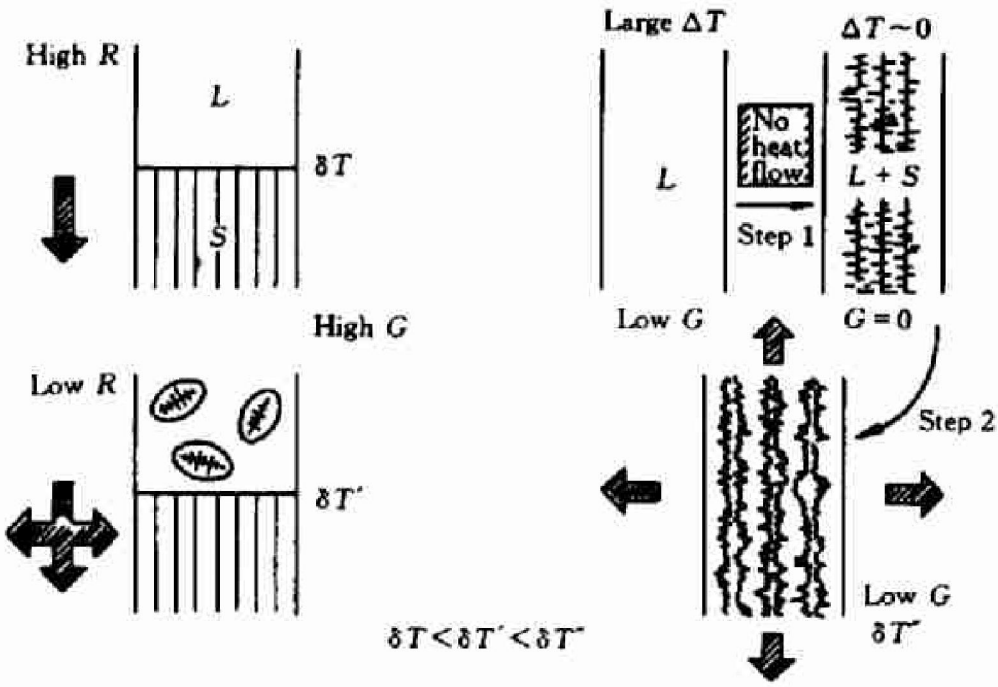

Fig. 4 Comparison between conventional directional solidification (a) and rapid directional solidification excited from supercooled melts (or SDS) (b)

L—Liquid; S—Solid; G—Temperature gradient; R—Pulling rate; δT—Interface supercooling; ΔT—Melt supercooling. The shadow arrow indicates the direction of heat flux.

heterogeneous and foreign nuclei in melt by evaporation and decomposition or dull and remove them by absorption with various kinds of glass cleaner in order to obtain deep supercooling of the melt. By taking the advantages of melt inheritance remelting of supercooled samples carried out in an inductor for D. S., the samples were controlled at a critical temperature of recalescence and then face-stimulated by using an exciting resource, the supercooled melt would be directionally solidified by a considerable driving force. The principle of the whole process is

shown in Fig.5.

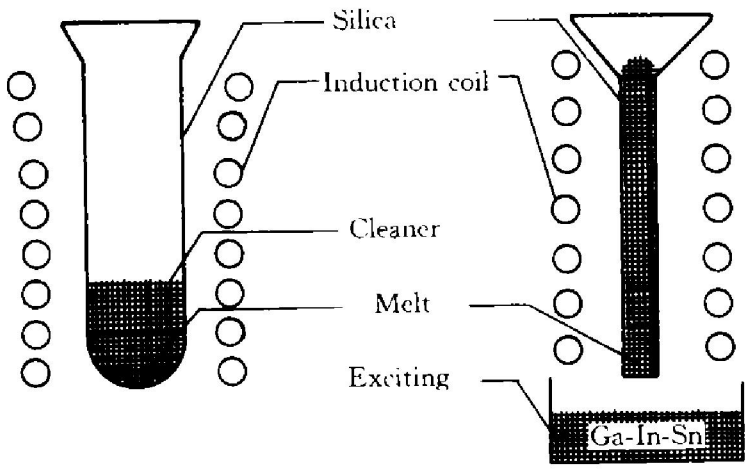

Fig.5 Principle of experiments of supercooling and supercooling solidification

3.2 Experimental results and discussion

3.2.1 Solidification microstructure of SDS samples

Fig.6 schematically shows the solidification structure of SDS. It can be seen that from the bottom(part of stimulated nucleation) to the top of the sample there appears in sequence fine equiaxed crystal →transient area →columnar dendrite →coarse equiaxed area, demonstrating the regularity of morphological evolution. Microstructure in columnar dendritic crystal area of SDS under various supercooling conditions in

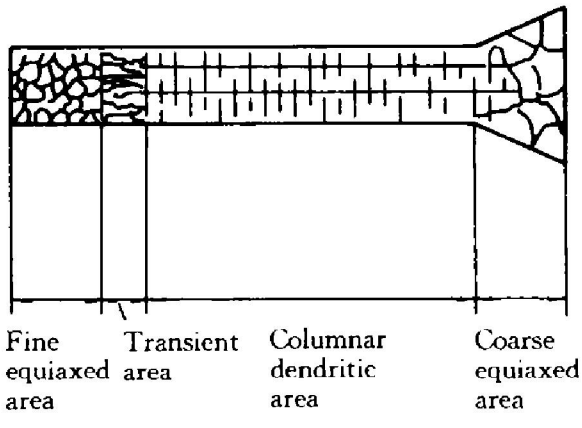

Fig.6 Diagram of microstructure of SDS samples

contrast with that of LMC is shown in Fig.7. It is shown that the dendritic structure by SDS is equivalent to that of LMC, its arm trunks are straight and fine, and the average deviation of crystal orientation from the axial line is about 5.8°; the primary arm spacing is a about 30 μm, and the secondary sidebranches degenerate significantly. According to the statistical results of experiments, the area of preferred columnar structure occupies about 60% of the whole length.

3.2.2 Solidification behavior

For the supercooled melt used for D. S. tests, glass cleaning and circular supercooling treatment are adopted for removing the heterogeneous and foreign nuclei. In the process of deep supercooling directional solidification, once the bottoms of sample is stimulated, the solidification can be completed very fast so as to avoid the occurrence of new nuclei in the melt, which may damage the uniaxial direction solidification. Besides, parts of latent heat transfers through the supercooled melt causing the supercooling to be gradually decreased, which means that the solidification rate is not a constant but depends on the relevant interface position.

3.2.2.1 Model of crystal growth

In the process of supercooling D.S., crystal growth is conducted in a supercooled melt. In general, dendrite growth is a fundamental mode for supercooled melt, but diffusionless solidification may also occur when the melt supercooling becomes large enough. From the aspect of interface morphology during solidification, diffusionless solidification asks the interface to be planar. Trivedi and Kurz[6] gave a criterion of absolute stability of planar interface in undercooled melt,

$$v_{\mathrm{abs}} = (v_{\mathrm{abs}})_C + (v_{\mathrm{abs}})_T \tag{2}$$

or

$$v_{\mathrm{abs}} = \frac{\Delta T_0 \times D}{\Gamma \times K} + \frac{\alpha_1 \times \Delta H}{\Gamma \times C_p} \tag{2'}$$

where α_1, ΔH and C_p are thermo-diffussion coefficient, latent crystallization heat, and specific heat, respectively; D, ΔT_0 and K are solute-diffussion coefficient, interval of solids and liquid at concentration of C_0 and equilibrium solute partition coefficient; and Γ is Gibbs-Thompson coefficient.

From Eq.(2), solid-liquid interface seems

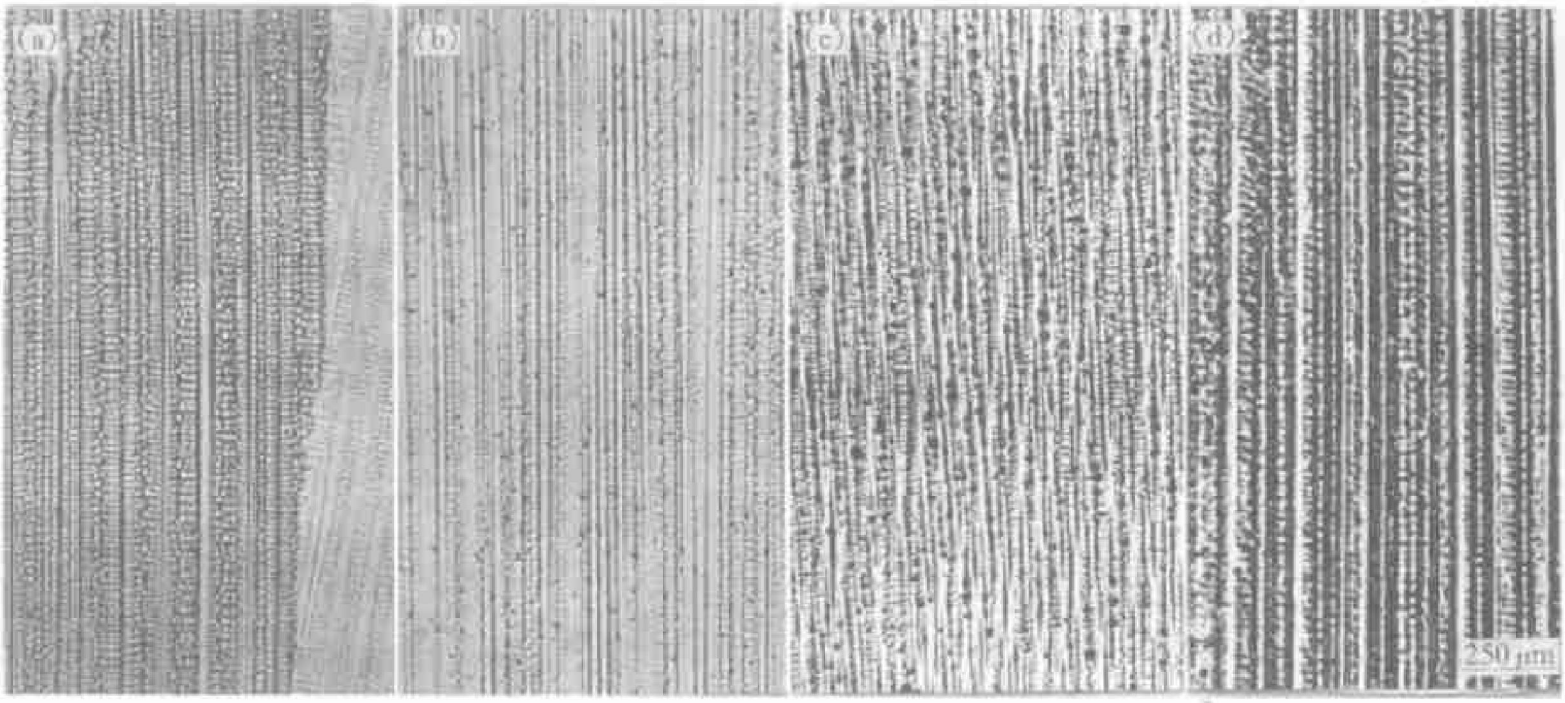

Fig.7 Microstructure of SDS samples in contrast with that of LMC
(a)—$\Delta T = 63$ K; (b)—$\Delta T = 136$ K;
(c)—$\Delta T = 158$ K; (d)—LMC($G_L = 250\ K\cdot cm^{-1}$, $v = 500\ \mu m\cdot s^{-1}$)

to be absolutely stable when growth rate $v > v_{abs}$, which leads the supercooled melt to solidify with planar interface, and solute trapping effect causes the melt to produce a diffusionless solidification under large supercooling. In fact, T-K theory was deduced with an assumption that the supercooling solidification is an adiabatic process, i.e, the temperature gradient at the interface in solid $G_S = 0$, which is not in agreement with practical condition of supercooling solidification process where $G_S > 0$. Considering $G_S > 0$ in solid and $G_L < 0$ in liquid in a supercooling D. S. process, the critical velocity of absolute stability of planar interface can be given as follows[7]:

$$v_{abs} = (v_{abs})_C + 2s(v_{abs})_T \quad (3)$$

where s is a stability parameter, which is a function of α and β, and it can be expressed by

$$s = \max\left\{\left|\frac{1}{Y^2}\left[2(\eta-1)\times\frac{-\alpha+}{-\alpha+(\alpha^2+\beta^2)^{1/2}+\beta+}\rightarrow\right.\right.$$
$$\left.\left.\leftarrow\frac{(\alpha^2+\beta^2)^{1/2}}{\beta(1+Y^2)^{1/2}}+2\eta\times\frac{\beta+}{-\alpha+(\alpha^2+\beta^2)^{1/2}+}\rightarrow\right.\right.$$
$$\left.\left.\leftarrow\frac{\beta(1+Y^2)^{1/2}}{\beta+\beta(1+Y^2)^{1/2}}\right]\right|\Big|_{\eta\cdot\alpha\cdot\beta}$$

where $\alpha = \alpha_L/\alpha_S$ (thermo-diffusion coefficient), $\beta = \beta_L/\beta_S$ (thermo-conductivity) and η is the fraction of latent heat released through supercooled melt.

According to the relation between latent heat fraction and stability parameters given by Ludwig, we have:

(a) $s = 0.5$ as $\eta = 1$, whole latent heat of solidification is released through supercooled melt, Eq. (3) will be degenerated to Eq. (2). Applying the data in Table 1, the critical velocity of absolute stability for planar interface v_{abs} is 4.3×10^3 m/s.

(b) $s = 0$ as $\eta = 0.5$, only half of latent heat is released through supercooled melt, Eq. (3) is retrograded to the form of M. S. theory, its critical velocity for absolute stability of planar interface v_{abs} is 0.28 m/s. So by the calculation given above, the range of the critical rate of the absolute planar interfacial stability is given as $v_{abs} = (0.28-4.3)\times10^3$ m/s. In other words, in directional deep supercooling solidification process the condition of segregation free solidification requires the growth rate to lie within the

v_{abs} range. However, the experimentally determined average solidification rate is approximately 0.53 cm/s, which is much smaller than the theoretical v_{abs}. Therefore, in directional deep supercooling solidification process, even though the crystal grows in a supercooled melt, the segregation free solidification will not occur. The crystal growth still takes the form of dendritic growth.

3.2.2.2 Modeling solidification process

In directional deep supercooling solidification process, the dendritic growth is carried out in a supercooled melt, so the growth rate is considered to be related to the supercooling temperature of the melt. Furthermore, the heat of fusion released through solid phase and supercooled melt also depends on the thermal-physical properties of the alloy.

Table 1 Thermodynamic properties used in calculations[8]

ΔH—Latent heat of fusion, 2.3×10^2 J·g^{-1}·K^{-1}
ΔS—Melting entropy, 1.344 J·cm^{-3}·K^{-1}
C_p—Specific heat of metal, 0.576 J·g^{-1}·K^{-1}
σ—Surface energy, 3.74×10^{-5} J·cm^{-2}
Γ—Surface tension, $=\sigma(\Delta S)^{-1}$ cm·K
σ^*—Stability constant, 0.025
D—Solute diffusivity coefficient, 3×10^{-5} cm^{-2}·s^{-1}
a—Thermal diffusivity coefficient, 3×10^{-2}cm^{-2}·s^{-1}

(a) Modeling of supercooling

Based on the LGK[9] theory, the functional relationship between the dendritic tip supercooling ΔT, dendritic tip radius R, and the growth rate v is given as

$$\Delta T = \Delta T_t + \Delta T_c + \Delta T_r \tag{4}$$

and

$$R = \frac{\Gamma/\sigma}{\frac{\Delta H}{C_p} \times P_t - \frac{mC_0(1-K_0)}{1-(1-K_0)I_V(P_C)} \times P_C} \tag{5}$$

using interactive and the data from Fig. 1, the single-value function relationship between ΔT—v can be determined and given in Fig. 8. The comparison of theoretically determined ΔT—v relationship by LGK theory with the average solidification rate obtained in experiments shows the same trends, but with relatively large discrepancies. The disagreements could be resulted from the change of the single valued relationship between ΔT and v caused by the release of the latent heat. In the SDS process, the latent heat causes the dendritic tip supercooling temperature to decrease, and the actual solidification rate is not a constant. The thermo-conductivity analysis is to be performed in the following.

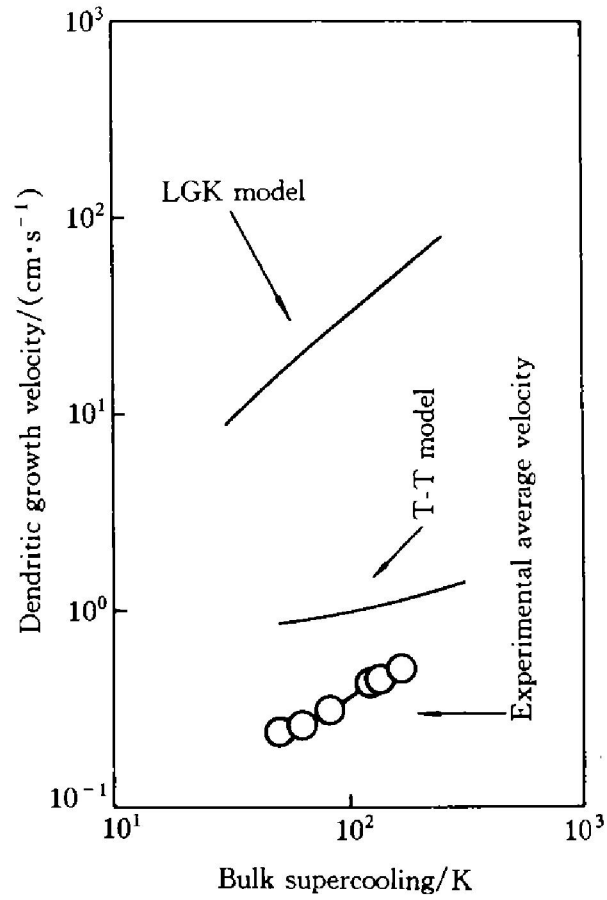

Fig.8 Solidification velocity vs supercooling

(b) Modeling of heat transfer

When crystals grow into the supercooled melt with v within unit time, the released latent heat noted as $\Delta H v \rho$ (where ρ is the alloy density, and ΔH is the alloy latent heat), could be transferred one dimensionally through the crystallized solid phase, as well as through the supercooled melt. The heat transfer mechanism is shown in Fig. 9.

The latent heat loss through the crystallized solid phase is

$$Q_S = K_S \times G_S \tag{6}$$

where K_S is the solid phase heat transfer coefficient, G_S given as $(T_r - T_0)/x$, is the solid phase temperature gradient.

The latent heat loss through supercooled melt is

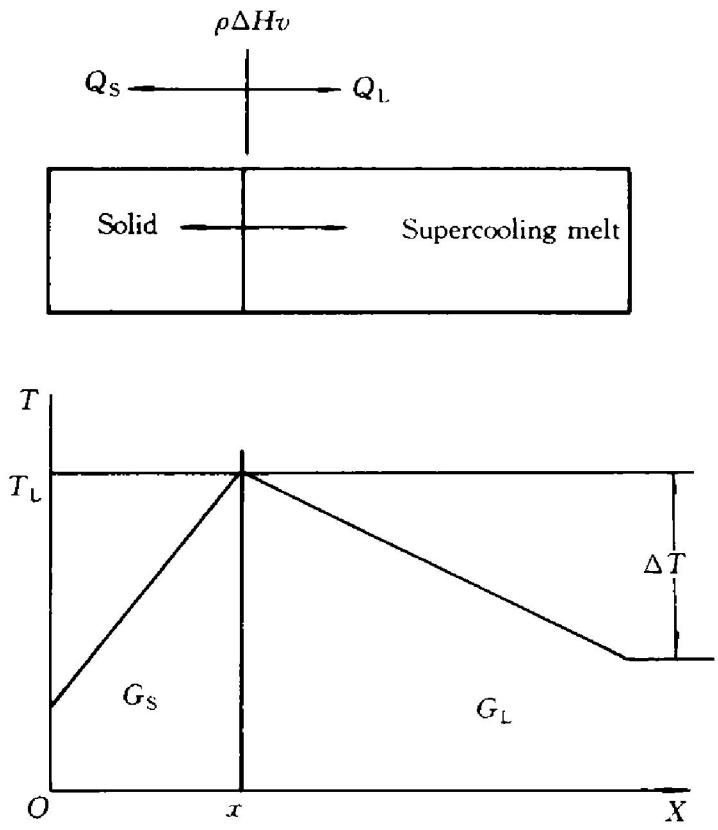

Fig. 9 Distribution of thermal unit and temperature in solidification interface

$$Q_L = K_L \times G_L \quad (7)$$

where K_L is the melt phase heat transfer coefficient; G_L, taking the form of $\Delta T/(l-x)$, is the temperature gradient in the melt.

From Eqs. (6) and (7), the thermal-equilibrium equation at the solidification interface can be derived,

$$\Delta H v \rho = K_S \times G_S + K_L \times G_L \quad (8)$$

rewriting Eq. 8, the solidification rate v can be written as

$$v = \frac{1}{\rho \times \Delta H} \times \left[K_S \times \frac{T_r - T_0}{x} + K_L \times \frac{\Delta T}{L - x} \right] \quad (9)$$

where ΔT—melt supercooling, K; x—distance from exciting source, mm; L—sample length, ≈ 50 mm; T_r—maximum recalescence temperature, K; T_0—medium temperature, K.

In order to make the theoretical calculation more convenient, the maximum recalescence temperature is set approximately equal to the liquidus temperature T_L, with $K_S = K_L = 3.52$ J/cm·s·K[10]. By utilizing the thermal-physical parameters of Cu-Ni alloy presented in Fig. 1, the solidification rate along the longitudinal direction of sample at certain supercooling temperature ($\Delta T = 150$ K) can be evaluated. The results are shown in Fig. 10(a). Fig. 10(b) is the plot of solidification rate versus the distance from the end of stimulation to the interface at different supercooling conditions. At $x = 1.5$ cm, the solidification rate does not change very much with the increase of the distance. Therefore, it is reasonable to conclude that the crystal growth has entered a stable growth regime. The relationship between the supercooling temperature and solidification rates is shown in Fig. 8.

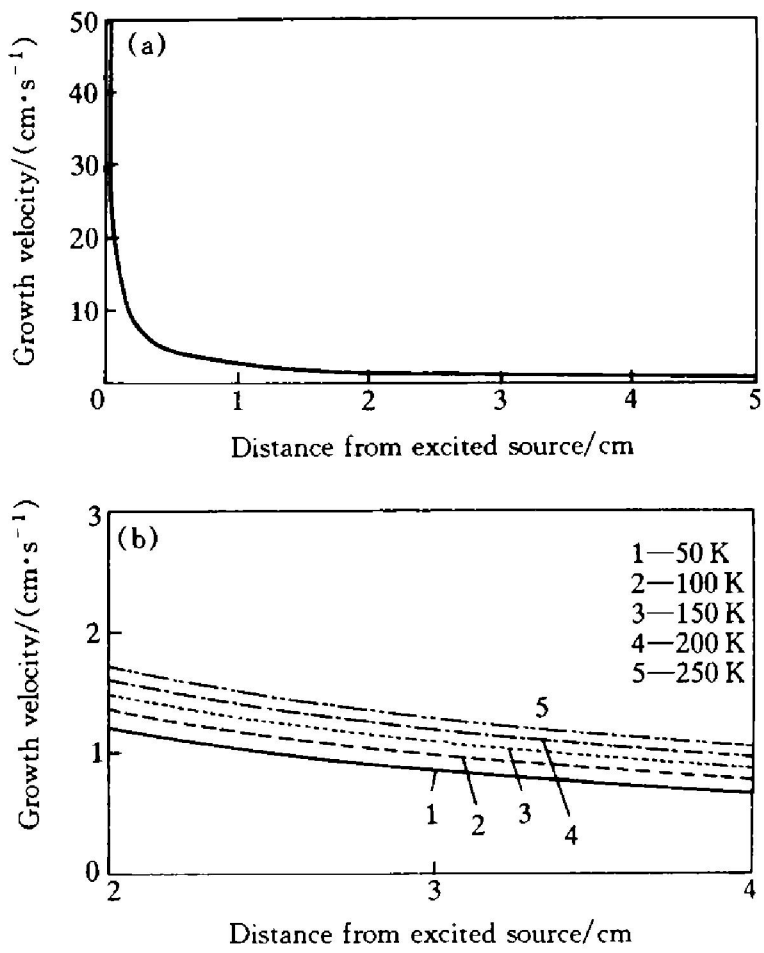

Fig. 10 Supercooling ΔT vs solidification velocity v (T-T Model)

The comparisons between the experimental and the T-T model's results indicate that:

First, the calculations from the T-T Model are in a much better agreement with the experimental results than those from LGK Model. Fig. 8 shows that from a semi-quantitative point of view, the T-T Model is capable of characterizing the relationship between the solidification

rates and the supercooling temperature under deep supercooling directional solidification.

Second, the T-T Model predicted that under certain supercooling condition, the crystal growth rate is not a constant, but a function of distance(from the S-L interface to the end stimulation). Their relationship is shown in Fig. 10 (a).

4 CONCLUSIONS

(1) There are substantial differences in the solidification characteristics between SDS and traditional directional solidification. Supercooled melt can be controlled to directionally solidify under reasonably controlled temperature and stimulated conditions.

(2) The microscopic structure under the directional deep supercooling solidification has four different character regions from the bottom to the top, i. e., fine equiaxed crystal area, transient area, columnar dendritic area and coarse equiaxed area.

(3) Columnar(dendritic) structure occupies over 60% of the total sample length. The primary arm spacing is about 30 μm, corresponding to that by LMC ($G_L = 250\ K \cdot cm^{-1}$, $v = 500\ \mu m \cdot s^{-1}$). The dendritic trunk appears straight and fine, and the deviation of dendritic orientation with axial direction is less than 5.8° in average.

(4) In directional deep supercooling solidification process, the solidification rates are much smaller than v_{abs}, therefore, the crystal growth takes the form of dendrite.

(5) A semi-quantitative T-T Model describing the solidification rate and supercooling temperature, has been established. The v—ΔT relationship predicted by the T-T Model is in good agreement with experimental results. The formation of fine equiaxed, transient and columnar region under the directional deep supercooling solidification can then be successfully explained by applying the v—ΔT—X relationship.

REFERENCES

1 Lux B , Haour G and Mollard F. Metall, 1981, 35: 1235.
2 Kiminami C S, Axmann W and Sahm P R. Journal of Materials Science Letters , 1989, 8: 201~203.
3 Stanescu J, Sahm P R, Schadlich-Stubenrauch J *et al*. In: 40 th Annual Technical Meeting: Investment Casting Institute, Las Vegas, 1992.
4 Xie Faqin, Zhang Jun, Mao Xieming *et al*. Journal of Materials Processing Technology, 1997, 63: 776~778.
5 Tiller W A, Jackson K A, Ruttur J W *et al*. Acta Metall, 1953, 1: 428.
6 Trivedi R and Kurz W. Acta Metall, 1986, 34: 1663.
7 Ludwig A. Acta Metall, 1991, 39: 2795~2798.
8 Herlach D M. Key Engineering Materials , 1993: 81~83, 89~94.
9 Lipton J, Glicksman M E and Kurz W. Mat Sci Eng, 1984, 65: 57~63.
10 Ma Qingfang *et al*. Practical Thermal-Physical Properties Manual. Beijing: China Agriculture Publishing House, 1986.

(Edited by Peng Chaoqun)